MPP-2003-48
PSI-PR-03-16
hep-ph/0310364



# Electroweak radiative corrections to deep-inelastic neutrino scattering — implications for NuTeV ?

K.-P. O. Diener[1], S. Dittmaier[2] and W. Hollik[2]

[1] *Paul-Scherrer-Institut, Würenlingen und Villigen*
*CH-5232 Villigen PSI, Switzerland*

[2] *Max-Planck-Institut für Physik (Werner-Heisenberg-Institut)*
*D-80805 München, Germany*

**Abstract:**
We calculate the $\mathcal{O}(\alpha)$ electroweak corrections to charged- and neutral-current deep-inelastic neutrino scattering off an isoscalar target. The full one-loop-corrected cross sections, including hard photonic corrections, are evaluated and compared to an earlier result which was used in the NuTeV analysis. In particular, we compare results that differ in input-parameter scheme, treatment of real photon radiation and factorization scheme. The associated shifts in the theoretical prediction for the ratio of neutral- and charged-current cross sections can be larger than the experimental accuracy of the NuTeV result.

October 2003

## 1 Introduction

Deep-inelastic neutrino scattering has been analyzed in the NuTeV experiment [ 1] with a rather high precision. In detail, the neutral- to charged-current cross-section ratios [ 2]

$$R^\nu = \frac{\sigma^\nu_{\rm NC}(\nu_\mu N \to \nu_\mu X)}{\sigma^\nu_{\rm CC}(\nu_\mu N \to \mu^- X)}, \qquad R^{\bar\nu} = \frac{\sigma^{\bar\nu}_{\rm NC}(\bar\nu_\mu N \to \bar\nu_\mu X)}{\sigma^{\bar\nu}_{\rm CC}(\bar\nu_\mu N \to \mu^+ X)} \tag{1.1}$$

have been measured to an accuracy of about 0.2% and 0.4%, respectively. In addition, the quantity

$$R^- = \frac{\sigma^\nu_{\rm NC}(\nu_\mu N \to \nu_\mu X) - \sigma^{\bar\nu}_{\rm NC}(\bar\nu_\mu N \to \bar\nu_\mu X)}{\sigma^\nu_{\rm CC}(\nu_\mu N \to \mu^- X) - \sigma^{\bar\nu}_{\rm CC}(\bar\nu_\mu N \to \mu^+ X)}, \tag{1.2}$$

as proposed by Paschos and Wolfenstein [ 3], has been considered. As a central result, the NuTeV collaboration has translated their measurement into a value for the on-shell weak mixing angle, $\sin^2\theta_{\rm W} = 1 - M^2_{\rm W}/M^2_{\rm Z}$, which can, thus, be viewed as an independent (but rather indirect) determination of the W- to Z-boson mass ratio. The NuTeV result on $\sin^2\theta_{\rm W}$ is, however, about $3\sigma$ away from the result obtained from the global fit [ 4] of the Standard Model (SM) to the electroweak precision data.

The $3\sigma$ difference of the NuTeV result to the SM global fit to data, together with the fact that the evaluation of the NuTeV measurement is very involved, triggered some discussion about the reliability of the NuTeV result. A detailed discussion of various experimental as well as theoretical issues can be found in Ref. [ 5], where in particular QCD corrections (see also Ref. [ 6] and references therein), charm-mass effects, and uncertainties from the parton distribution functions have been considered. According to Ref. [ 5], none of these issues seems to be a candidate for an error or an underestimate of uncertainties in the analysis. However, the authors of Ref. [ 5] pointed out that the inclusion of electroweak radiative corrections, which influences the result significantly, is based on a single calculation [ 7] only[1] and that a careful recalculation of these corrections is desirable.

In this paper we present such a calculation of the $\mathcal{O}(\alpha)$ electroweak corrections to neutral- and charged-current deep-inelastic neutrino scattering off an isoscalar target. Apart from a different set of parton densities and input parameters the most important difference between our calculation and the result of Ref. [ 7] lies in the treatment of initial-state mass singularities due to collinear radiation of a photon from the incoming quark.

The input parameters used for the numerical analysis of Ref. [ 7] are not completely specified and, in order to fix all free parameters of the electroweak SM, need to be supplemented by fermion masses that we obtained from references quoted within Ref. [ 7]. A comparison of numerical results should therefore be interpreted with care. In any case, the effect on the electroweak corrections on the NuTeV results should be further analyzed. We will provide a Fortran code that could be used for an update of the NuTeV data analysis.

The paper is organized as follows. In Section 2 we set our conventions, define the necessary kinematical quantities, and consider the lowest-order cross sections. Section 3

[1] Electroweak radiative corrections to neutral-current-induced neutrino deep-inelastic scattering were also investigated in Ref. [ 8], but the corresponding hadronic cross sections were not evaluated numerically.

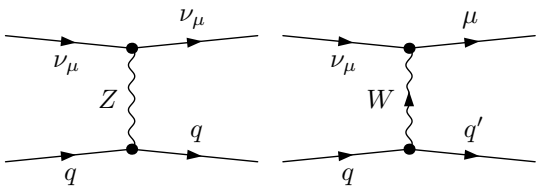


Figure 1: Lowest-order diagrams for $\nu_\mu q \to \nu_\mu q$ and $\nu_\mu q \to \mu^- q'$ scattering

contains an overview over the structure of the calculated electroweak corrections, a description of the calculational framework, and explicit results on some specific one-loop corrections; particular attention is paid to the treatment of collinear photon radiation and the related fermion-mass singularities. Our numerical results are presented in Section 4. Section 5 contains a short summary.

## 2 Conventions and lowest-order cross sections

We consider the neutral-current (NC) and charged-current (CC) parton processes

$$\text{NC:} \quad \nu_\mu(p_l) + q(p_q) \quad \to \quad \nu_\mu(k_l) + q(k_q), \qquad q = \mathrm{u}, \mathrm{d}, \mathrm{s}, \mathrm{c}, \bar{\mathrm{u}}, \bar{\mathrm{d}}, \bar{\mathrm{s}}, \bar{\mathrm{c}}, \tag{2.1}$$

$$\text{CC:} \quad \nu_\mu(p_l) + q(p_q) \quad \to \quad \mu^-(k_l) + q'(k_q), \qquad q = \mathrm{d}, \mathrm{s}, \bar{\mathrm{u}}, \bar{\mathrm{c}}, \quad q' = \mathrm{u}, \mathrm{c}, \bar{\mathrm{d}}, \bar{\mathrm{s}}, \tag{2.2}$$

and the processes with all particles replaced by their antiparticles. The assignment of momenta is indicated in parentheses. At lowest order the former processes proceed via Z-boson exchange, the latter via W-boson exchange; the corresponding Feynman diagrams are shown in Figure 1. The diagrams and results for incoming antiquarks can be obtained from those of incoming quarks by crossing the external quark lines. CP symmetry implies that the (parton) cross sections for $\nu_\mu$–quark and $\nu_\mu$–antiquark scattering are equal to the ones of $\bar{\nu}_\mu$–antiquark and $\bar{\nu}_\mu$–quark scattering, respectively. In the following we neglect the muon mass and the parton masses whenever possible. The quark masses are only kept as regulators for mass singularities, which appear as mass logarithms in the (photonic) corrections; the issue of quark-mass logarithms will be discussed below in detail. The muon mass is not only required as regulator for collinear final-state radiation but also for a proper description of forward scattering in the (loop-induced) $\gamma\nu_\mu\bar{\nu}_\mu$ vertex, as described below as well. The Mandelstam variables of the partonic processes are defined as

$$\begin{aligned} s &= (p_l + p_q)^2 = 4E^2, \\ t &= (p_l - k_l)^2 = -2E^2(1 - \cos\theta), \\ u &= (p_q - k_l)^2 = -2E^2(1 + \cos\theta), \end{aligned} \tag{2.3}$$

where $E$ and $\theta$ denote the beam energy and scattering angle in the partonic centre-of-mass (CM) frame. Moreover, we introduce the variable

$$y = -\frac{t}{s} = \frac{1}{2}(1 - \cos\theta). \tag{2.4}$$

The momentum of the incoming (anti-)quark $q$ is related to the total nucleon momentum $P_N$ by the usual scaling relation

$$p_q^\mu = x P_N^\mu, \tag{2.5}$$

which holds in the CM frame of the partonic system where the nucleon mass $M_N$ is negligible. The variable $x$ is the usual momentum fraction, restricted by $0 < x < 1$. Since deep-inelastic neutrino scattering usually is accessed in fixed-target experiments (as NuTeV), we take the energy $E_\nu^{\rm LAB}$ of the incoming (anti-)neutrino beam to define the incoming momentum $p_l$ in the rest frame of the nucleon, called LAB in the following. Thus, the scattering energy $E$ and the variable $s$ are given by

$$s = 4E^2 = 2xM_N E_\nu^{\rm LAB}, \tag{2.6}$$

up to terms of higher order in the nucleon mass. Neglecting the nucleon mass, there is also a simple relation between the scattering angle $\theta$ in the partonic CM frame (or equivalently $y$) and the energy $E_{\rm had}^{\rm LAB}$ of the outgoing quark in the LAB frame,

$$E_{\rm had}^{\rm LAB} = \frac{E_\nu^{\rm LAB}}{2}(1-\cos\theta) = yE_\nu^{\rm LAB}. \tag{2.7}$$

$E_{\rm had}^{\rm LAB}$ can be identified as the energy deposited by hadrons in the detector. More generally, a momentum with components $K^\mu$ in the CM frame receives the following components in the LAB system,

$$\begin{aligned} K^\mu_{\rm LAB} &= \Big(\gamma(K^0+\beta K^3), K^1, K^2, \gamma(\beta K^0 + K^3)\Big) \\ &\qquad \text{with} \quad \gamma \sim \sqrt{E_\nu^{\rm LAB}/(2xM_N)}, \quad \beta \to 1. \end{aligned} \tag{2.8}$$

Note that the asymptotic expressions for $\gamma$ and $\beta$ are fully sufficient and can be consistently used; deviations from the full Lorentz boost are suppressed by nucleon-mass terms.

The lowest-order matrix elements corresponding to the tree diagrams of Figure 1 can be easily worked out; the result is

$$\begin{aligned} \mathcal{M}^\tau_{\rm NC,0} &= \frac{e^2 g^\tau_{qqZ} g^-_{\nu_\mu\nu_\mu Z}}{t-M_{\rm Z}^2}\,\Big[\bar u(k_l)\,\gamma^\rho\,\omega_- u(p_l)\Big]\,\Big[\bar u(k_q)\,\gamma_\rho\,\omega_\tau u(p_q)\Big], \\ \mathcal{M}^\tau_{\rm CC,0} &= \frac{e^2 g^-_{q'qW} g^-_{\nu_\mu\mu W}}{t-M_{\rm W}^2}\,\Big[\bar u(k_l)\,\gamma^\rho\,\omega_- u(p_l)\Big]\,\Big[\bar u(k_{q'})\,\gamma_\rho\,\omega_- u(p_q)\Big], \end{aligned} \tag{2.9}$$

where $\omega_\pm = \frac{1}{2}(1\pm\gamma_5)$ denote the chirality projectors and an obvious notation for the Dirac spinors $u(p_q)$, etc., is used. The index $\tau = \pm$ indicates the chirality of the incoming quark. The coupling factors are given by

$$g^\tau_{q'qW} = \frac{V_{q'q}}{\sqrt{2}s_{\rm w}}\,\delta_{\tau-}, \qquad g^\tau_{\nu_\mu\mu W} = \frac{1}{\sqrt{2}s_{\rm w}}\,\delta_{\tau-}, \qquad g^\tau_{ffZ} = -\frac{s_{\rm w}}{c_{\rm w}}Q_f + \frac{I_f^3}{c_{\rm w}s_{\rm w}}\,\delta_{\tau-}, \tag{2.10}$$

where $Q_f$ and $I_f^3 = \pm 1/2$ are the relative charge and the third component of the weak isospin of fermion $f$, respectively. The weak mixing angle is fixed by the mass ratio $M_{\rm W}/M_{\rm Z}$, according to the on-shell condition $\sin^2\theta_W \equiv s_W^2 = 1-c_W^2 = 1-M_{\rm W}^2/M_{\rm Z}^2$. Note that the CKM matrix element for the $q'q$ transition, $V_{q'q}$, appears only as global factor $|V_{q'q}|^2$ in the CC cross section. Thus, in the limit of vanishing final-state quark masses, the factors $|V_{q'q}|^2$ add up to one after the sum over the flavours of $q'$ is taken.

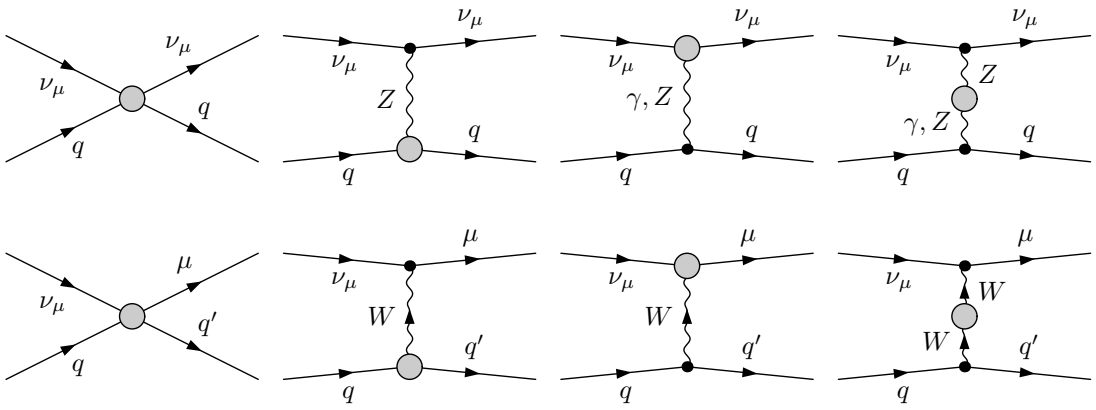


Figure 2: Generic diagrams for the one-loop corrections to $\nu_\mu q \to \nu_\mu q$ and $\nu_\mu q \to \mu^- q'$.

## 3 Calculation of radiative corrections

### 3.1 Overview and calculational framework

We have calculated the cross sections to the processes (2.1) and (2.2) including relative $\mathcal{O}(\alpha)$ electroweak corrections. This means our partonic cross sections $\sigma$ can be written as a sum of leading-order ($\sigma_0$), virtual ($\sigma_{\rm virt}$), and real ($\sigma_{\rm real}$) contributions:

$$\sigma = \sigma_0 + \sigma_{\rm virt} + \sigma_{\rm real} = \sigma_0(1+\delta), \tag{3.1}$$

where $\delta$ denotes the relative correction. The virtual correction $\sigma_{\rm virt}$ contains one-loop diagrams and counterterms,

$$\sigma_{\rm virt} = \sigma_{\rm one-loop} + \sigma_{\rm ct}. \tag{3.2}$$

The generic diagrams for these contributions, with loops and counterterms summarized by the blobs, are shown in Figure 2. Within the real correction $\sigma_{\rm real}$ we can discriminate bremsstrahlung corrections ($\sigma_{\rm brem}$) and a counterterm contribution ($\sigma_{\rm coll}$) that accounts for the absorption of initial-state mass singularities into the parton densities,

$$\sigma_{\rm real} = \sigma_{\rm brem} + \sigma_{\rm coll}. \tag{3.3}$$

The bremsstrahlung diagrams are shown in Figure 3.

The contributions to $\sigma_{\rm virt}$ and $\sigma_{\rm real}$ diverge individually and cannot be evaluated unless suitable regularization and renormalization prescriptions are employed. All parts of our calculation have been performed in two independent ways, resulting in two completely independent computer codes. Both loop calculations are carried out in 't Hooft–Feynman gauge and are based on the standard techniques for one-loop integrations as, e.g., described in Refs. [ 9, 10]. Ultraviolet divergences are treated in dimensional regularization and eliminated using the on-shell renormalization scheme [ 10, 11] in the formulation of Ref. [ 10]. Infrared (i.e. soft and collinear) singularities are regularized by an infinitesimal photon mass and small fermion masses. The artificial photon-mass dependence of the virtual and (soft) real corrections cancels in the sum of both contributions, according to Bloch and Nordsieck [ 12]. The role of the other fermion-mass singularities will be discussed below.

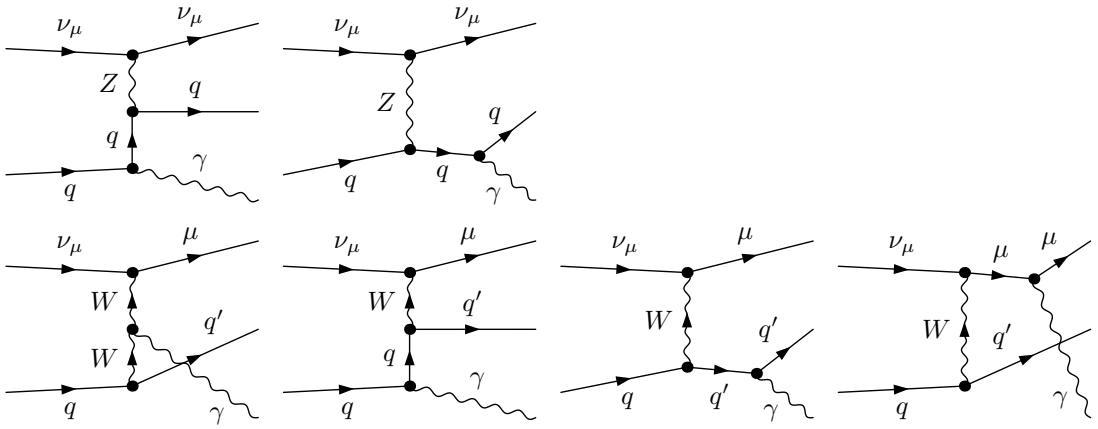


Figure 3: Bremsstrahlung diagrams for the processes $\nu_\mu q \to \nu_\mu q$ and $\nu_\mu q \to \mu^- q'$.

In detail, the two calculations of the $\mathcal{O}(\alpha)$ corrections have been performed as follows:

1. In the first calculation, the fully differential partonic $2 \to 2, 3$ particle cross sections have been obtained with the Mathematica packages FeynArts [ 13] and FormCalc [ 14]. The one-loop integrals are evaluated with the LoopTools library [ 14]. The combination of virtual and real corrections is done by phase-space slicing in the soft-photon region, i.e. soft photons are excluded from the phase-space integral of the bremsstrahlung by a small energy cutoff $\Delta E < E_\gamma$ and added as correction factor to the lowest-order cross section derived from the eikonal current (see e.g. Refs. [ 10, 12]). In the whole calculation, fermion masses are kept small but non-zero in the matrix elements and in the phase space.

2. The second calculation is completely independent of the first. The results for the CC processes (2.2) are obtained via crossing the results of Ref. [ 15] where the related Drell–Yan-like process $q\bar{q}' \to l^- \bar{\nu}_l$ was treated in $\mathcal{O}(\alpha)$. Of course, the W-boson width, needed there to describe the W-boson resonance, is set to zero in our case. The corrections to the NC processes (2.1) have been calculated in the same way as described in Ref. [ 15] for the CC case. This means that the one-loop amplitudes are generated with FeynArts [ 13] and algebraically reduced using FeynCalc [ 16] or own independent Mathematica routines; the scalar and tensor one-loop integrals are evaluated using the methods and results of Refs. [ 9, 10]. The bremsstrahlung amplitudes are derived in the Weyl–van der Waerden spinor technique, following the formulation of Ref. [ 17]. The combination of virtual and real corrections is performed in three different ways: using two different versions of phase-space slicing, which are described in Ref. [ 15] in detail, and the dipole subtraction approach, as described in Ref. [ 18]. Using these techniques, masses of the external fermions can be set to zero in all bremsstrahlung amplitudes consistently; the mass dependence relevant for mass-singular regions is restored according to factorization properties of amplitudes.

We have checked that the different calculations lead to results on the relative $\mathcal{O}(\alpha)$ corrections to the NC and CC cross sections that typically agree within $\sim 0.1\%$. For the

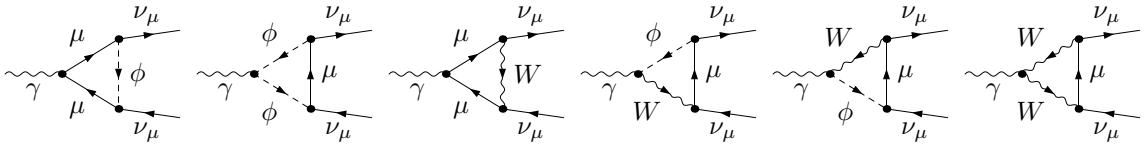


Figure 4: Diagrams for the one-loop correction to the $\gamma\nu_\mu\bar{\nu}_\mu$ vertex.

$\mathcal{O}(\alpha)$-induced shift $\Delta\sin^2\theta_\mathrm{W}$ in the weak mixing angle (see Section 4.1 below) we find agreement within $\sim 0.0003$. The residual differences, which are due to the various ways of treating the fermion-mass effects, are thus below the NuTeV theoretical uncertainties related to other effects [ 1, 5].

In the following, we do not present the full formulas for all contributions to the cross section[2], since their derivation is by now a standard exercise and their form does not reveal further insight. We restrict ourselves to sketching salient features and delicate parts.

### 3.2 Contributions from 2-particle final states – tree level and virtual corrections

The differential cross section including all $2 \to 2$ particle contributions at $\mathcal{O}(\alpha^3)$ is given by

$$\frac{\mathrm{d}\sigma}{\mathrm{d}\cos\theta} = \frac{1}{2}\,\frac{1}{32\pi s}\sum_{\tau=\pm}\left(|\mathcal{M}_0^\tau|^2 + 2\,\mathrm{Re}\{(\mathcal{M}_0^\tau)^*\mathcal{M}_1^\tau\}\right), \tag{3.4}$$

where $\mathcal{M}_0$ and $\mathcal{M}_1$ are the amplitudes at tree and one-loop level, respectively. Note that rotational invariance has been used to integrate over the azimuthal angle $\phi$, leading to a global factor $2\pi$, and the explicit prefactor $1/2$ accounts for the spin average of the initial-state quark.

Among the virtual corrections, there are two contributions to the NC processes that become numerically delicate in the limit of small momentum transfer ($t \to 0$): the $\gamma\nu_\mu\bar{\nu}_\mu$ vertex correction and the $\gamma Z$ mixing self-energy, indicated in the last two generic diagrams in the first line of Figure 2. The corresponding contributions to the relative correction $\delta$ read

$$\delta^\tau_{\gamma\nu_\mu\bar{\nu}_\mu} = -\frac{4s_\mathrm{w}c_\mathrm{w}Q_q}{g^\tau_{qqZ}}\frac{t-M_\mathrm{Z}^2}{t}\left[F_{\gamma\nu_\mu\bar{\nu}_\mu}(t) + \frac{1}{4s_\mathrm{w}c_\mathrm{w}}\delta Z_{Z\gamma}\right], \tag{3.5}$$

$$\delta^\tau_{\gamma Z} = \frac{2Q_q}{g^\tau_{qqZ}}\left[\frac{\Sigma_\mathrm{T}^{\gamma Z}(t)}{t} + \frac{1}{2}\delta Z_{\gamma Z} + \frac{t-M_\mathrm{Z}^2}{2t}\delta Z_{Z\gamma}\right], \tag{3.6}$$

where $\Sigma_\mathrm{T}^{\gamma Z}$ is the transversal part of the unrenormalized $\gamma Z$ mixing self-energy and $\delta Z_{\gamma Z}$ and $\delta Z_{Z\gamma}$ are the renormalization constants for the mixing of the $\gamma$ and $Z$ fields. The precise definition and explicit expressions for these quantities in 't Hooft–Feynman gauge can be found in Ref. [ 10]. The one-loop diagrams contributing to the $\gamma\nu_\mu\bar{\nu}_\mu$ vertex are depicted in Figure 4, where $\phi$ represents the would-be Goldstone field corresponding to the W boson. The renormalized vertex form factor $F^\mathrm{ren}_{\gamma\nu_\mu\bar{\nu}_\mu}(t)$, which is given by the expression

[2]For the CC processes all contributions can be obtained from the formulas of Ref. [ 15] via crossing.

in square brackets in Eq. (3.5), explicitly reads

$$
\begin{aligned}
F^{\mathrm{ren}}_{\gamma\nu_\mu\bar{\nu}_\mu}(t) &= -\frac{\alpha}{16\pi s_{\mathrm{w}}^2}\Bigg\{\frac{2(m_\mu^2+2M_{\mathrm{W}}^2)}{M_{\mathrm{W}}^2} - 4[B_0(0,M_{\mathrm{W}},M_{\mathrm{W}}) - B_0(t,M_{\mathrm{W}},M_{\mathrm{W}})] \\
&\quad - \frac{2m_\mu^4 + 2m_\mu^2M_{\mathrm{W}}^2 - 4M_{\mathrm{W}}^4 + m_\mu^2 t - 6M_{\mathrm{W}}^2 t}{tM_{\mathrm{W}}^2} \\
&\quad \times [B_0(t,m_\mu,m_\mu) - B_0(t,M_{\mathrm{W}},M_{\mathrm{W}})] \\
&\quad + \frac{2(m_\mu^6 - 3m_\mu^2M_{\mathrm{W}}^4 + 2M_{\mathrm{W}}^6 + m_\mu^4 t - 2m_\mu^2M_{\mathrm{W}}^2 t + 4M_{\mathrm{W}}^4 t)}{tM_{\mathrm{W}}^2} \\
&\quad \times [C_0(0,t,0,m_\mu,M_{\mathrm{W}},M_{\mathrm{W}}) + C_0(0,t,0,M_{\mathrm{W}},m_\mu,m_\mu)] \\
&\quad + 4tC_0(0,t,0,M_{\mathrm{W}},m_\mu,m_\mu)\Bigg\}. \qquad (3.7)
\end{aligned}
$$

The definitions and general results for the scalar 2- and 3-point integrals $B_0$ and $C_0$ can be found in Ref. [ 10]. Note that the full muon mass dependence is kept in this formula. For large $|t|$, i.e. for $|t| \gg m_\mu^2$, the muon mass can be neglected; in this limit the form factor reads

$$
\begin{aligned}
F^{\mathrm{ren}}_{\gamma\nu_\mu\bar{\nu}_\mu}(t)\Big|_{m_\mu=0} &= -\frac{\alpha}{16\pi s_{\mathrm{w}}^2}\Bigg\{4 - 4[B_0(0,M_{\mathrm{W}},M_{\mathrm{W}}) - B_0(t,M_{\mathrm{W}},M_{\mathrm{W}})] \\
&\quad + \frac{2(2M_{\mathrm{W}}^2+3t)}{t}[B_0(t,0,0) - B_0(t,M_{\mathrm{W}},M_{\mathrm{W}})] \\
&\quad + \frac{4M_{\mathrm{W}}^2(M_{\mathrm{W}}^2+2t)}{t}[C_0(0,t,0,0,M_{\mathrm{W}},M_{\mathrm{W}}) + C_0(0,t,0,M_{\mathrm{W}},0,0)] \\
&\quad + 4tC_0(0,t,0,M_{\mathrm{W}},0,0)\Bigg\}, \qquad (3.8)
\end{aligned}
$$

which reproduces the full expression for $F_{\gamma\nu_\mu\bar{\nu}_\mu}$ up to terms of $\mathcal{O}(m_\mu^2/t)$ and $\mathcal{O}(m_\mu^2/M_{\mathrm{W}}^2)$. For small $|t|$, the general expression (3.7) becomes numerically unstable, because the whole expression in this limit is of $\mathcal{O}(t)$ while individual terms involve constants and even $1/t$ poles. A stable result for this limit can be obtained by performing an asymptotic expansion for large $M_{\mathrm{W}}$; this leads to

$$
\begin{aligned}
F^{\mathrm{ren}}_{\gamma\nu_\mu\bar{\nu}_\mu}(t) \quad \widetilde{M_{\mathrm{W}}\to\infty} \quad & -\frac{\alpha}{36\pi M_{\mathrm{W}}^2 s_{\mathrm{w}}^2}\Bigg\{6m_\mu^2[B_0(0,m_\mu,m_\mu) - B_0(t,m_\mu,m_\mu)] \\
& - t[2 - 3B_0(0,M_{\mathrm{W}},M_{\mathrm{W}}) + 3B_0(t,m_\mu,m_\mu)]\Bigg\}, \qquad (3.9)
\end{aligned}
$$

which is valid up to terms of $\mathcal{O}(m_\mu^4/M_{\mathrm{W}}^4)$, $\mathcal{O}(m_\mu^2 t/M_{\mathrm{W}}^4)$, and $\mathcal{O}(t^2/M_{\mathrm{W}}^4)$. From this expression one can easily obtain the limit $t \to 0$ for the contribution of the $\gamma\nu_\mu\bar{\nu}_\mu$ vertex to the relative correction,

$$
\delta^\tau_{\gamma\nu_\mu\bar{\nu}_\mu}\Big|_{t=0} = \frac{Q_q}{g^\tau_{qqZ}}\frac{\alpha}{3\pi c_{\mathrm{w}} s_{\mathrm{w}}}\Bigg\{1 + \ln\Big(\frac{M_{\mathrm{W}}^2}{m_\mu^2}\Big)\Bigg\}. \qquad (3.10)
$$

In the limit $t \to 0$, the relative correction induced by $\gamma Z$ mixing tends to the value

$$
\delta^\tau_{\gamma Z}\Big|_{t=0} = \frac{2Q_q}{g^\tau_{qqZ}}\left[\frac{\Sigma_{\mathrm{T}}^{\gamma Z}(0) - \Sigma_{\mathrm{T}}^{\gamma Z}(M_{\mathrm{Z}}^2)}{M_{\mathrm{Z}}^2} + \Sigma_{\mathrm{T}}^{\gamma Z\prime}(0)\right], \qquad (3.11)
$$

where $\Sigma_{\rm T}^{\gamma Z\prime}(t)$ is the derivative of $\Sigma_{\rm T}^{\gamma Z}(t)$ w.r.t. the variable $t$. Since the derivative $\Sigma_{\rm T}^{\gamma Z\prime}(0)$ numerically results from $[\Sigma_{\rm T}^{\gamma Z}(t)-\Sigma_{\rm T}^{\gamma Z}(0)]/t$ for $t \to 0$, the actual evaluation of $\delta_{\gamma Z}^{\tau}$ deserves some care for small $|t|$. This is, however, less tricky than for $\delta_{\gamma\nu_\mu\bar{\nu}_\mu}^{\tau}$, since only one power of $t$ effectively cancels for $t \to 0$. A peculiarity in $\Sigma_{\rm T}^{\gamma Z\prime}(0)$ is that it involves logarithms $\ln(m_f/M_{\rm Z})$ of all charged fermions $f$. These contributions result from the $\gamma Z$ mixing in the non-perturbative domain of small momentum transfer. Thus, the light-quark masses entering here should be tuned in such a way that the hadronic $\gamma Z$ mixing, which can be obtained via dispersion relations [ 19], is reproduced. This highly non-trivial task is, however, beyond the scope of this paper.

In the actual numerical evaluation, we proceed in the two following ways (corresponding to the two independent calculations described under the same labels in Section 3.1):

1. In the first calculation we substitute $\delta_{\gamma\nu_\mu\bar{\nu}_\mu}^{\tau}\Big|_{t=0}$ and $\delta_{\gamma Z}^{\tau}\Big|_{t=0}$ for the exact $t$-dependent expression if $|t| < 5 \times 10^{-3}\,\mathrm{GeV}^2$.

2. In the second calculation the asymptotic formulas (3.8) or (3.9) are used if $|t|$ is larger or smaller than $1\,\mathrm{GeV}^2$, respectively. At the matching point, these two formulas agree within about 4 digits. The $\gamma Z$ mixing part is evaluated with the full expression (3.5) everywhere.

### 3.3 Contributions from 3-particle final states – bremsstrahlung corrections

For the real photonic corrections, the processes (2.1) and (2.2) have to be considered with an additional photon (with momentum $k$) in the final state. The contribution $\sigma_{\rm brem}$ of these radiative processes to the parton cross section are given by

$$\sigma_{\rm brem} = \frac{1}{2}\frac{1}{2\hat{s}} \int \mathrm{d}\Gamma_\gamma \sum_{\rm spins} |\mathcal{M}_\gamma|^2, \tag{3.12}$$

where $\mathcal{M}_\gamma$ is the corresponding amplitude and the phase-space integral is defined by

$$\int \mathrm{d}\Gamma_\gamma = \int \frac{\mathrm{d}^3\mathbf{k}_l}{(2\pi)^3 2k_{l,0}} \int \frac{\mathrm{d}^3\mathbf{k}_q}{(2\pi)^3 2k_{q,0}} \int \frac{\mathrm{d}^3\mathbf{k}}{(2\pi)^3 2k_0}\, (2\pi)^4 \delta(p_l + p_q - k_l - k_q - k). \tag{3.13}$$

The phase-space integral (3.12) diverges in the soft ($k_0 \to 0$) and collinear ($p_q k, k_q k \to 0$, and $k_l k \to 0$ in the CC case) regions logarithmically if the photon and fermion masses are set to zero. For the treatment of the soft and collinear singularities we have applied the phase-space slicing method as well as a subtraction approach, as mentioned above.

### 3.4 Hadron cross section and redefinition of parton densities

The neutrino–nucleus scattering cross section $\sigma_{\nu N}$ is obtained from the parton cross sections $\sigma$ by convolution with the corresponding parton distribution functions $q(x)$,

$$\sigma_{\nu N}(E_\nu^{\rm LAB}) = \sum_q \int_0^1 \mathrm{d}x\, q_{\rm iso}(x)\, \sigma(p_l, p_q), \tag{3.14}$$

where $x$ is the momentum fraction carried by the parton $q$ and $M$ is the factorization scale. The squared CM energy $s$ of the partonic process is related to the neutrino energy

$E_\nu^{\rm LAB}$ in the LAB frame according to Eq.(2.6). In the sum $\sum_q$ the variable $q$ runs over the incoming quarks and antiquarks indicated in Eqs. (2.1) and (2.2). The subscript "iso" indicates that we average over the parton densities for an (anti-)quark $q$ in the proton and neutron, $q(x) \equiv f_q^{\rm p}(x)$ and $f_q^{\rm n}(x)$,

$$q_{\rm iso}(x) = \frac{1}{2}\left(f_q^{\rm p}(x) + f_q^{\rm n}(x)\right). \tag{3.15}$$

Owing to isospin invariance ($f_{\rm u}^{\rm p}(x) \equiv f_{\rm d}^{\rm n}(x)$, etc.), this is equivalent to an isospin average of the parton densities of the proton, ${\rm u}_{\rm iso}(x) \equiv {\rm d}_{\rm iso}(x) \equiv \frac{1}{2}({\rm u}(x) + {\rm d}(x))$, etc.

The $\mathcal{O}(\alpha)$-corrected parton cross section $\sigma$ contains mass singularities of the form $\alpha \ln(m_q)$, which are due to collinear photon radiation off the initial-state quarks. In complete analogy to the $\overline{\rm MS}$ factorization scheme for next-to-leading order QCD corrections, we absorb these collinear singularities into the quark distributions. This is achieved by replacing $q(x)$ in (3.14) according to

$$\begin{aligned} q(x) \;\;\to\;\; & q(x,M^2) \\ & - \int_x^1 \frac{{\rm d}z}{z}\, q\Big(\frac{x}{z}, M^2\Big)\, \frac{\alpha}{2\pi}\, Q_q^2 \left\{ \ln\Big(\frac{M^2}{m_q^2}\Big) \Big[P_{ff}(z)\Big]_+ - \Big[P_{ff}(z)\Big(2\ln(1-z)+1\Big)\Big]_+ \right\}, \end{aligned} \tag{3.16}$$

where $M$ is the factorization scale (see Ref. [ 15]). This replacement defines the same finite parts in the $\mathcal{O}(\alpha)$ correction as the usual $\overline{\rm MS}$ factorization in $D$-dimensional regularization for exactly massless partons, where the $\ln(m_q)$ terms appear as $1/(D-4)$ poles. In (3.16) we have regularized the soft-photon pole by using the $[\ldots]_+$ prescription. This procedure is fully equivalent to the application of a soft-photon cutoff $\Delta E$ (see Ref. [ 20]) where

$$\begin{aligned} q(x) \;\;\to\;\; & q(x,M^2) \left[ 1 - \frac{\alpha}{\pi}\, Q_q^2 \left\{ 1 - \ln(2\Delta E/\sqrt{\hat{s}}) - \ln^2(2\Delta E/\sqrt{\hat{s}}) \right.\right. \\ & \left.\left. + \left(\ln(2\Delta E/\sqrt{\hat{s}}) + \frac{3}{4}\right) \ln\left(\frac{M^2}{m_q^2}\right) \right\} \right] \\ & - \int_x^{1-2\Delta E/\sqrt{\hat{s}}} \frac{dz}{z}\, q\left(\frac{x}{z}, M^2\right)\, \frac{\alpha}{2\pi}\, Q_q^2\, P_{ff}(z) \left\{ \ln\left(\frac{M^2}{m_q^2} \frac{1}{(1-z)^2}\right) - 1 \right\}. \end{aligned} \tag{3.17}$$

The convolution of the correction terms to the parton densities [r.h.s. of Eqs. (3.16) or (3.17)] with the lowest-order cross section $\sigma_0$ defines the "collinear counterterm" contribution $\sigma_{\rm coll}$ in the real photonic correction $\sigma_{\rm real}$, as defined in Eq. (3.3).

The absorption of the collinear singularities of $\mathcal{O}(\alpha)$ into quark distributions, as a matter of fact, requires also the inclusion of the corresponding $\mathcal{O}(\alpha)$ corrections into the DGLAP evolution of these distributions and into their fit to experimental data. At present, this full incorporation of $\mathcal{O}(\alpha)$ effects in the determination of the quark distributions has not yet been performed. However, an approximate inclusion of the $\mathcal{O}(\alpha)$ corrections to the DGLAP evolution shows [ 21] that the impact of these corrections on the quark distributions in the $\overline{\rm MS}$ factorization scheme is smaller than remaining QCD

uncertainties; this is also supported by a recent analysis of the MRST collaboration [ 22] who took into account the $\mathcal{O}(\alpha)$ effects to the DGLAP equations.[3]

### 3.5 Structure of divergences in the radiative corrections

While ultraviolet divergences are absorbed by renormalization and soft singularities always compensate between virtual and (soft) real corrections, the issue of collinear singularities is more delicate. These singularities originate from collinear photon emission off the external fermions and lead to mass logarithms $\alpha \ln m_f$. As described in the previous section, the $\alpha \ln m_q$ terms from initial-state radiation are absorbed into the parton distribution functions.

However, there are also $\alpha \ln m_{q'}$ and (in the CC case) $\alpha \ln m_\mu$ terms from final-state radiation. According to the Kinoshita–Lee–Nauenberg (KLN) theorem [ 23], these terms drop out if the final state is treated sufficiently inclusive, i.e. if the cones for quasi-collinear photon emission around the charged outgoing fermions are fully integrated over. This condition is, in general, not fulfilled if phase-space cuts at the parton level are applied. For instance, restricting the outgoing hadronic energy, $E^{\mathrm{LAB}}_{\mathrm{had,min}} < E^{\mathrm{LAB}}_{\mathrm{had}} < E^{\mathrm{LAB}}_{\mathrm{had,max}}$, spoils the inclusiveness w.r.t. photon emission collinear to the outgoing quark, so that corrections proportional to $\alpha \ln m_{q'}$ survive. On the other hand, a cut on the total hadronic+photonic energy, $E^{\mathrm{LAB}}_{\mathrm{had+phot,min}} < E^{\mathrm{LAB}}_{\mathrm{had+phot}} < E^{\mathrm{LAB}}_{\mathrm{had+phot,max}}$, which is equivalent to cutting the outgoing lepton energy, destroys the inclusiveness w.r.t. collinear photon emission of muons in the CC processes, leading to $\alpha \ln m_\mu$ corrections. Both types of mass singularities are avoided if *photon recombination* in the final state is taken into account before applying selection cuts.

For instance, a simple recombination scheme is provided by the following algorithm:

1. For an event with a photon in the final state, the smallest angle $\theta_{\gamma f}$ between the outgoing photon and the outgoing fermions ($q$ for NC; $\mu$ or $q'$ for CC) is determined in the LAB frame.

2. If $\theta_{\gamma f} < \theta_{\mathrm{cut}}$, the photon is recombined with the nearest fermion $f$. This means that the momenta of the photon and of the fermion $f$ are added and assigned to the new "quasi-fermion" $\tilde{f}$; then the photon is discarded from the event.

3. Finally, we impose the hadronic energy cut $E^{\mathrm{LAB}}_{\mathrm{had,recomb}} > 10\,\mathrm{GeV}$, where "recomb" indicates that the momentum after possible recombination is used.

This procedure is "collinear safe" with respect to initial-state and final-state collinear singularities, i.e. photons that are nearly collinear to a charged fermion are treated inclusively. Note that photons exactly collinear to the initial-state quark receive zero momentum in the LAB frame, which effectively acts as recombination with the initial state. All final-state muon and quark-mass logarithms cancel in the corresponding integrated cross section. The collinear safety of observables can be ideally checked by comparing results

[3]Note that the inclusion of $\mathcal{O}(\alpha)$ effects in the DGLAP evolution also leads to a photon distribution function in the nucleon. The impact of the resulting $\nu_\mu\gamma$ reactions, which are connected to the bremsstrahlung corrections via crossing, is, however, expected to be very small owing to smallness of the induced photon distribution.

obtained with phase-space slicing to the ones obtained with a subtraction technique; we have performed this comparison and find agreement within the integration errors. In the numerical evaluation we take $\theta_{\rm cut} = 5^\circ$.

Although all of the above cuts are idealizations, the cut on the sum $E^{\rm LAB}_{\rm had+phot}$ of hadronic and photonic energies seems to be most appropriate for a fixed-target experiment where all but the energy of neutrinos and muons is deposited in a calorimeter.

## 4 Discussion of results

### 4.1 The quantities $\delta R^\nu$ and $\Delta \sin^2\theta_W$

Although the electroweak $\mathcal{O}(\alpha)$ corrections to the NC and CC cross sections represent the central results of this paper, it is useful to translate them into a correction to the cross-section ratio $R^\nu = \sigma^\nu_{\rm NC}/\sigma^\nu_{\rm CC}$ introduced in Eq. (1.1) and to make contact to its interpretation in terms of an effective shift in the on-shell weak mixing angle.

Writing $\delta\sigma$ for the correction to the cross section, the (first-order) correction $\delta R^\nu$ to the ratio $R^\nu$ reads

$$\delta R^\nu = R^\nu \left( \frac{\delta\sigma^\nu_{\rm NC}}{\sigma^\nu_{\rm NC}} - \frac{\delta\sigma^\nu_{\rm CC}}{\sigma^\nu_{\rm CC}} \right) = R^\nu \left( \delta R^\nu_{\rm NC} + \delta R^\nu_{\rm CC} \right). \tag{4.1}$$

Following Ref. [ 7], the quantities

$$\delta R^\nu_{\rm NC} = \frac{\delta\sigma^\nu_{\rm NC}}{\sigma^\nu_{\rm NC}}, \qquad \delta R^\nu_{\rm CC} = -\frac{\delta\sigma^\nu_{\rm CC}}{\sigma^\nu_{\rm CC}} \tag{4.2}$$

have been defined for later convenience.

In order to define an effective shift $\Delta \sin^2\theta_{\rm W}$, we quote the approximate relation [ 2]

$$R^\nu \sim \frac{1}{2} - \sin^2\theta_{\rm W} + \frac{20}{27}\sin^4\theta_{\rm W}, \tag{4.3}$$

which results from the lowest-order neutrino deep-inelastic scattering cross section ratio for isoscalar targets upon neglecting the momentum transfers in the W- and Z-boson propagators. The correction $\delta R^\nu$ can be interpreted as a correction $\delta \sin^2\theta_{\rm W}$ in the variable $\sin^2\theta_{\rm W}$,

$$\delta R^\nu \sim \delta \left( \frac{1}{2} - \sin^2\theta_{\rm W} + \frac{20}{27}\sin^4\theta_{\rm W} \right) = \left( -1 + \frac{40}{27}\sin^2\theta_{\rm W} \right) \delta \sin^2\theta_{\rm W}. \tag{4.4}$$

As done in Ref. [ 7], we define the shift $\Delta \sin^2\theta_{\rm W}$ as the negative of the correction $\delta \sin^2\theta_{\rm W}$. Combining the above relations, we are, thus, lead to

$$\begin{aligned} \Delta \sin^2\theta_{\rm W} \equiv -\delta \sin^2\theta_{\rm W} &\equiv \frac{\frac{1}{2} - \sin^2\theta_{\rm W} + \frac{20}{27}\sin^4\theta_{\rm W}}{1 - \frac{40}{27}\sin^2\theta_{\rm W}} \left( \frac{\delta\sigma^\nu_{\rm NC}}{\sigma^\nu_{\rm NC}} - \frac{\delta\sigma^\nu_{\rm CC}}{\sigma^\nu_{\rm CC}} \right) \\ &= \frac{\frac{1}{2} - \sin^2\theta_{\rm W} + \frac{20}{27}\sin^4\theta_{\rm W}}{1 - \frac{40}{27}\sin^2\theta_{\rm W}} \left( \delta R^\nu_{\rm NC} + \delta R^\nu_{\rm CC} \right). \end{aligned} \tag{4.5}$$

### 4.2 Input parameters

If not stated otherwise, we used the following set of input parameters [ 24] for the numerical evaluation,

$$\begin{aligned}
&G_\mu = 1.16639\times10^{-5}\,\text{GeV}^{-2}, \quad \alpha(0) = 1/137.03599976, \quad \alpha(M_Z) = 1/128.930,\\
&M_N = m_\text{p} = 0.938271998\,\text{GeV},\\
&M_\text{W} = 80.423\,\text{GeV}, \qquad M_\text{Z} = 91.1876\,\text{GeV}, \qquad M_\text{H} = 115\,\text{GeV},\\
&m_\text{e} = 0.510998902\,\text{MeV}, \qquad m_\mu = 105.658357\,\text{MeV}, \qquad m_\tau = 1.77699\,\text{GeV},\\
&m_\text{u} = 66\,\text{MeV}, \qquad m_\text{c} = 1.2\,\text{GeV}, \qquad m_\text{t} = 174.3\,\text{GeV},\\
&m_\text{d} = 66\,\text{MeV}, \qquad m_\text{s} = 150\,\text{MeV}, \qquad m_\text{b} = 4.3\,\text{GeV}.
\end{aligned} \tag{4.6}$$

The masses of the light quarks are adjusted such as to reproduce the hadronic contribution to the photonic vacuum polarization of Ref. [ 25]. They are relevant only for the evaluation of the charge renormalization constant in the $\alpha(0)$-scheme and for the small correction induced by the $\gamma Z$ mixing at zero-momentum transfer [see Eq. (3.11)]. For the calculation of the $\nu_\mu N$ cross sections we have set the energy of the incoming neutrino to $E_\nu^\text{LAB} = 80\,\text{GeV}$ and adopted the CTEQ4L parton distribution functions [ 26]. The factorization scale $M$ is derived from the leptonic momentum transfer, i.e. it is set to $M = \sqrt{-(p_l - k_l)^2}$ (with the momenta after possible photon recombination).

For the explicit evaluation and the following numerical discussion we distinguish three different input-parameter schemes

- $\alpha(0)$-*scheme:* The fine-structure constant $\alpha(0)$ and all particle masses define the complete input (i.e. $\alpha(M_\text{Z})$ and $G_\mu$ are not used). In this scheme, the relative corrections to the cross sections sensitively depend on the light quark masses via $\alpha \ln m_q$ terms that enter the charge renormalization.

- $\alpha(M_\text{Z})$-*scheme:* The effective electromagnetic coupling $\alpha(M_\text{Z})$ and all particle masses define the complete input (i.e. $\alpha(0)$ and $G_\mu$ are not used). Tree-level couplings are derived from $\alpha(M_\text{Z})$, and the relative corrections are related by $\delta_{\alpha(M_\text{Z})-\text{scheme}} = \delta_{\alpha(0)-\text{scheme}} - 2\Delta\alpha(M_\text{Z})$, where $\Delta\alpha(Q)$ accounts for the running of the electromagnetic coupling from scale $Q = 0$ to $Q = M_\text{Z}$ (induced by light fermions) and cancels the corresponding $\alpha \ln m_q$ terms in $\delta_{\alpha(0)-\text{scheme}}$.

- $G_\mu$-*scheme:* The Fermi constant $G_\mu$ and all particle masses define the complete input (i.e. $\alpha(0)$ and $\alpha(M_\text{Z})$ are not used). Tree-level couplings are derived from the effective coupling $\alpha_{G_\mu} = \sqrt{2}G_\mu M_\text{W}^2 s_\text{w}^2/\pi$, and the relative corrections are related by $\delta_{G_\mu-\text{scheme}} = \delta_{\alpha(0)-\text{scheme}} - 2\Delta r$, where $\Delta r$ contains the radiative corrections to muon decay and is defined [ 27] by

$$M_\text{W}^2\left(1 - \frac{M_\text{W}^2}{M_\text{Z}^2}\right) = \frac{\pi\alpha}{\sqrt{2}G_\mu}\frac{1}{1-\Delta r(\alpha, M_\text{W}, M_\text{Z}, M_\text{H}, m_f)}. \tag{4.7}$$

  In the following we consistently use $\Delta r$ at the one-loop level, as, for instance, explicitly given in Ref. [ 10]. Since $\Delta\alpha(M_\text{Z})$ is contained in $\Delta r$, there is no large effect induced by the running of the electromagnetic coupling in the $G_\mu$-scheme either.

More details about the various schemes can, e.g., be found in Refs. [ 10, 11, 15].

Hadronic energy cut: $E_{\rm had}^{\rm LAB} > 10\,\text{GeV}$

| IPS | $R_0^\nu$ | $\delta R_{\rm NC}^\nu$ | $\delta R_{\rm CC}^\nu$ | $\Delta \sin^2\theta_{\rm W}$ |
|---|---|---|---|---|
| $\alpha(0)$ | 0.31766(2) | 0.0582(1) | −0.0758(4) | −0.0082(2) |
| $\alpha(M_{\rm Z})$ | 0.31766(2) | −0.0639(1) | 0.0452(4) | −0.0088(2) |
| $G_\mu$ | 0.31766(2) | 0.0003(1) | −0.0185(4) | −0.0085(2) |

Hadronic+photonic energy cut: $E_{\rm had+phot}^{\rm LAB} > 10\,\text{GeV}$

| IPS | $R_0^\nu$ | $\delta R_{\rm NC}^\nu$ | $\delta R_{\rm CC}^\nu$ | $\Delta \sin^2\theta_{\rm W}$ |
|---|---|---|---|---|
| $\alpha(0)$ | 0.31766(2) | 0.0589(1) | −0.0842(4) | −0.0118(2) |
| $\alpha(M_{\rm Z})$ | 0.31766(2) | −0.0632(1) | 0.0363(4) | −0.0126(2) |
| $G_\mu$ | 0.31766(2) | 0.0011(1) | −0.0272(4) | −0.0122(2) |

Hadronic energy cut after $\gamma$ recombination: $E_{\rm had,recomb}^{\rm LAB} > 10\,\text{GeV}$

| IPS | $R_0^\nu$ | $\delta R_{\rm NC}^\nu$ | $\delta R_{\rm CC}^\nu$ | $\Delta \sin^2\theta_{\rm W}$ |
|---|---|---|---|---|
| $\alpha(0)$ | 0.31766(2) | 0.05861(1) | −0.07702(2) | −0.00863(1) |
| $\alpha(M_{\rm Z})$ | 0.31766(2) | −0.06349(1) | 0.04392(2) | −0.00917(1) |
| $G_\mu$ | 0.31766(2) | 0.00077(2) | −0.01980(2) | −0.00892(1) |

Table 1: Results on the ratio $R^\nu$ in lowest order ($R_0^\nu$), corrections from NC and CC cross sections ($\delta R_{\rm NC}^\nu$ and $\delta R_{\rm CC}^\nu$), and shift $\Delta \sin^2\theta_{\rm W}$, for various input-parameter schemes (IPS) and using different treatments of real photons in the final state. The number in parentheses indicates the statistical integration error in the last digit.

### 4.3 Numerical results

Using the input defined in the previous section, we have evaluated the corrections $\delta R_{\rm NC}^\nu$ and $\delta R_{\rm CC}^\nu$, as well as the corresponding shift $\Delta \sin^2\theta_{\rm W}$, in the various input-parameter schemes and for different treatments of photons in the final state. The corresponding numerical results are collected in Table 1.

We observe a large scheme dependence of the corrections $\delta R_{\rm NC}^\nu$ and $\delta R_{\rm CC}^\nu$ owing to the shifts of $-2\Delta\alpha(M_{\rm Z}) \sim -12\%$ and $-2\Delta r \sim -6\%$ in the relative corrections $\delta_{\alpha(M_{\rm Z})-\text{scheme}}$ and $\delta_{G_\mu-\text{scheme}}$, respectively, relative to the $\alpha(0)$-scheme. Since these shifts are identical in the NC and CC cross sections, they drop out in $\Delta \sin^2\theta_{\rm W}$. The remaining very small scheme dependence in $\Delta \sin^2\theta_{\rm W}$ is due to the different choice of the coupling $\alpha$ in the schemes, i.e. of formal two-loop order.

Moreover, Table 1 reveals that different ways of treating real photons in the final state selection lead to sizeable differences in the correction $\delta R_{\rm CC}^\nu$ to the CC cross section while $\delta R_{\rm NC}^\nu$ hardly changes. The differences can be explained by inspecting final-state radiation w.r.t. their inclusiveness. The variant $E_{\rm had+phot}^{\rm LAB} > 10\,\text{GeV}$, where the energy cut is applied to the sum of hadronic and photonic energy, is the only choice in which the collinear cone for radiation off outgoing muons is not treated inclusively, leading to logarithmically enhanced corrections proportional to $\alpha \ln m_\mu$. Numerically this effect changes $\delta R_{\rm CC}^\nu$ by $\sim 0.008$, and thus increases the shift $\Delta \sin^2\theta_{\rm W}$ by $\sim 0.004$. On the other hand, the variant

$E_{\rm had}^{\rm LAB} > 10\,\text{GeV}$, where the energy cut is applied to the bare outgoing quark energy, is the only case in which final-state quark logarithms $\alpha \ln m_q$ (in the NC case) or $\alpha \ln m_{q'}$ (in the CC case) are present. Numerically these effects turn out to be of the order $\sim 0.001$ in $\delta R^{\nu}_{\rm NC}$ and $\delta R^{\nu}_{\rm CC}$, and thus do not influence $\Delta \sin^2\theta_{\rm W}$ very much.

### 4.4 Comparison with existing results

Finally, we compare our results with the ones of the older calculation of Ref. [ 7] as far as possible. To this end, we adopt the (obsolete) input parameters of Ref. [ 7] which are, however, unfortunately not completely specified there.[4] The following parameters are explicitly given:

$$\begin{aligned} &\alpha(0) = 1/137.036, \quad \frac{\pi\alpha(0)}{\sqrt{2}G_\mu} = (37.281\,\text{GeV})^2, \quad \sin^2\theta_{\rm W} = 0.227, \\ &M_{\rm Z} = 93.8\,\text{GeV}, \qquad M_{\rm H} = 100\,\text{GeV}, \qquad m_{\rm t} = 180\,\text{GeV}. \end{aligned} \tag{4.8}$$

Neither the W-boson mass nor the masses of fermions other than the top quark are given in Ref. [ 7]. We supplement the above input parameters by the following fermion masses,

$$\begin{aligned} &M_N = m_{\rm p} = 0.938271998\,\text{GeV}, \\ &m_{\rm e} = 0.5110034\,\text{MeV}, \qquad m_\mu = 0.10565943\,\text{GeV}, \quad m_\tau = 1.7842\,\text{GeV}, \\ &m_{\rm u} = 80\,\text{MeV}, \qquad m_{\rm c} = 1.5\,\text{GeV}, \\ &m_{\rm d} = 80\,\text{MeV}, \qquad m_{\rm s} = 0.30\,\text{GeV}, \qquad m_{\rm b} = 4.5\,\text{GeV}. \end{aligned} \tag{4.9}$$

In detail, the lepton masses are taken from Ref. [ 28] and the quark masses from Ref. [ 29]; Ref. [ 7] indirectly refers to these papers.

The authors of Ref. [ 7] advocate the on-mass-shell renormalization scheme with the fine-structure constant $\alpha(0)$, the Fermi constant $G_\mu$, the Z- and Higgs-boson masses $M_{\rm Z}$ and $M_{\rm H}$, and all fermion masses as physical input parameters. In contrast to the conventional on-shell scheme the W-boson mass $M_{\rm W}$ is not an input parameter but is instead determined by (iterative) solution of the implicit relation (4.7). Using the above input parameters, except for $\sin^2\theta_W$, and solving Eq. (4.7) for $M_{\rm W}$ we find for the W-boson mass $M_{\rm W} = 83.807\,\text{GeV}$, which leads to $s_{\rm w}^2 = \sin^2\theta_{\rm W} = 0.2017$. This constitutes roughly a 10% discrepancy to the value $\sin^2\theta_{\rm W} = 0.227$ given in Ref. [ 7]; it is not clear where the latter is actually used in Ref. [ 7]. Having specified $M_{\rm W}$, we further assume that the authors of Ref. [ 7] proceed as in our $G_\mu$ scheme, i.e. by taking $G_\mu$ and all particle masses as input.

Concerning the treatment of initial-state quark-mass singularities, there is a conceptual difference between the calculation of Ref. [ 7] and ours. The authors of Ref. [ 7] do not apply $\overline{\rm MS}$ factorization, as we do, but instead set the masses $m_q$ of the incoming quarks to $m_q = xM_N$ without any additional subtractions. Moreover, the (rather old set of) parton distribution functions used in Ref. [ 7] are not available to us; the corrections, however, should depend on the parton densities only very weakly.

In Table 2 we compare our results with the ones quoted in Ref. [ 7]. Since the input is not completely clear, we use different setups. Specifically, we apply the usual $G_\mu$-scheme

[4] The full set of input parameters used in Ref. [ 7] could also not be provided by the authors on request.

Hadronic energy cut: $E_{\rm had}^{\rm LAB} > 10\,\text{GeV}$

| IPS | FS | $R_0^\nu$ | $\delta R_{\rm NC}^\nu$ | $\delta R_{\rm CC}^\nu$ | $\Delta \sin^2\theta_{\rm W}$ |
|---|---|---|---|---|---|
| result of Ref. [ 7] | BD | – | −0.0021 | −0.0223 | −0.0114 |
| $G_\mu$ | $\overline{\rm MS}$ | 0.31455(1) | 0.0010(1) | −0.0202(4) | −0.0090(2) |
| $G_\mu$($M_{\rm W}$ derived) | $\overline{\rm MS}$ | 0.33113(2) | −0.0018(1) | −0.0186(4) | −0.0095(2) |
| $G_\mu$ | BD | 0.31455(1) | −0.0026(1) | −0.0184(4) | −0.0098(2) |
| $G_\mu$($M_{\rm W}$ derived) | BD | 0.33113(2) | −0.0050(1) | −0.0169(4) | −0.0103(2) |

Hadronic+photonic energy cut: $E_{\rm had+phot}^{\rm LAB} > 10\,\text{GeV}$

| IPS | FS | $R_0^\nu$ | $\delta R_{\rm NC}^\nu$ | $\delta R_{\rm CC}^\nu$ | $\Delta \sin^2\theta_{\rm W}$ |
|---|---|---|---|---|---|
| $G_\mu$ | $\overline{\rm MS}$ | 0.31455(1) | 0.0018(1) | −0.0294(4) | −0.0130(2) |
| $G_\mu$($M_{\rm W}$ derived) | $\overline{\rm MS}$ | 0.33113(2) | −0.0010(1) | −0.0271(4) | −0.0132(2) |
| $G_\mu$ | BD | 0.31455(1) | −0.0018(1) | −0.0276(4) | −0.0138(2) |
| $G_\mu$($M_{\rm W}$ derived) | BD | 0.33113(2) | −0.0043(1) | −0.0253(4) | −0.0139(2) |

Hadronic energy cut after $\gamma$ recombination: $E_{\rm had,recomb}^{\rm LAB} > 10\,\text{GeV}$

| IPS | FS | $R_0^\nu$ | $\delta R_{\rm NC}^\nu$ | $\delta R_{\rm CC}^\nu$ | $\Delta \sin^2\theta_{\rm W}$ |
|---|---|---|---|---|---|
| $G_\mu$ | $\overline{\rm MS}$ | 0.31455(1) | 0.00138(2) | −0.02149(2) | −0.00943(1) |
| $G_\mu$($M_{\rm W}$ derived) | $\overline{\rm MS}$ | 0.33113(2) | −0.00139(2) | −0.01970(2) | −0.00988(1) |
| $G_\mu$ | BD | 0.31455(1) | −0.00214(2) | −0.01969(2) | −0.01023(1) |
| $G_\mu$($M_{\rm W}$ derived) | BD | 0.33113(2) | −0.00465(2) | −0.01805(2) | −0.01064(1) |

Table 2: Comparison with results of Ref. [ 7].

(denoted "$G_\mu$"), where $M_{\rm W} = 82.469\,\text{GeV}$ is calculated from $\sin^2\theta_{\rm W} = 0.227$ and $M_{\rm Z}$, as well as a modified $G_\mu$ scheme [denoted "$G_\mu$ ($M_{\rm W}$ derived)"] that differs from the former in the value of $M_{\rm W} = 83.807$, which is calculated from $G_\mu$ and the particle masses via $\Delta r$ at one loop. Moreover, we apply two different factorization schemes, the $\overline{\rm MS}$ scheme and the one used in Ref. [ 7] (quoted as "BD"). Of course, this comparison of results can neither prove nor disprove the correctness of the results of Ref. [ 7]. However, the first part of the table ($E_{\rm had}^{\rm LAB} > 10\,\text{GeV}$) suggests significant differences in the correction $\Delta \sin^2\theta_{\rm W}$. In any case, the variations in the corrections that are due to the different factorization schemes ($\overline{\rm MS}$ versus BD) and due to different ways of including the final-state photon in the hadronic energy in the final state can be as large as the accuracy in the NuTeV experiment, which is about 0.0016 in $\sin^2\theta_{\rm W}$ (if statistical and systematic errors are combined quadratically).

## 5 Summary

Results from a new calculation of electroweak $\mathcal{O}(\alpha)$ corrections to neutral- and charged-current neutrino deep-inelastic scattering have been presented. The salient features of the calculation and some delicate points of the corrections, such as the issue of

collinear fermion-mass singularities, have been discussed in detail. Unfortunately a tuned comparison to older results, which were used in the NuTeV data analysis, is not possible. However, a comparison based on an assumption for missing input parameters leaves room for speculating on possible significant differences in the electroweak radiative corrections. Therefore, an update of the NuTeV analysis seems to be desirable. We provide a Fortran code for the electroweak radiative corrections that could be used in this task. Specifically, our investigation of the factorization-scheme dependence for initial-state radiation and of different ways to treat photons in the final state reveals that these effects can be as large as the $3\sigma$ difference between the NuTeV measurement and the Standard Model prediction in the on-shell weak mixing angle.

A careful re-assessment of all theoretical uncertainties involved in the NuTeV analysis should be worked out, based on the new studies of both QCD [ 5, 6] and electroweak corrections. The NuTeV collaboration estimated the theoretical uncertainty due to missing higher-order effects to 0.00005 and 0.00011 in $\delta R^\nu$ and $\Delta \sin^2\theta_W$, respectively. The results on electroweak corrections presented in this paper indicate that these numbers are too optimistic.

## Acknowledgments

One of the authors (K. D.) would like to thank Michael Spira and Ansgar Denner for useful discussions. Dima Bardin is gratefully acknowledged for providing further information on Ref. [ 7]. This work was supported in part by the European Union under contract HPRN-CT-2000-00149.

## References

[1] G. P. Zeller *et al.* [NuTeV Collaboration], Phys. Rev. Lett. **88** (2002) 091802 [Erratum-ibid. **90** (2003) 239902] [hep-ex/0110059].

[2] C. H. Llewellyn Smith, Nucl. Phys. B **228** (1983) 205.

[3] E. A. Paschos and L. Wolfenstein, Phys. Rev. D **7** (1973) 91.

[4] M. W. Grünewald, hep-ex/0304023.

[5] K. S. McFarland and S. O. Moch, hep-ph/0306052.

[6] S. Davidson, S. Forte, P. Gambino, N. Rius and A. Strumia, JHEP **0202** (2002) 037 [hep-ph/0112302];
P. Gambino, hep-ph/0211009;
S. A. Kulagin, Phys. Rev. D **67** (2003) 091301 [hep-ph/0301045];
S. Kretzer and M. H. Reno, hep-ph/0307023;
B. A. Dobrescu and R. K. Ellis, hep-ph/0310154.

[7] D. Y. Bardin and V. A. Dokuchaeva, *On The Radiative Corrections To The Neutrino Deep Inelastic Scattering*, JINR-E2-86-260.

[8] W. J. Marciano and A. Sirlin, Phys. Rev. D **22** (1980) 2695 [Erratum-ibid. D **31** (1985) 213].

[9] G. 't Hooft and M. Veltman, Nucl. Phys. B **153** (1979) 365;
G. Passarino and M. Veltman, Nucl. Phys. B **160** (1979) 151;
W. Beenakker and A. Denner, Nucl. Phys. B **338** (1990) 349;
A. Denner, U. Nierste and R. Scharf, Nucl. Phys. B **367** (1991) 637.

[10] A. Denner, Fortsch. Phys. **41** (1993) 307.

[11] M. Böhm, H. Spiesberger and W. Hollik, Fortsch. Phys. **34** (1986) 687;
W. F. Hollik, Fortsch. Phys. **38** (1990) 165.

[12] F. Bloch and A. Nordsieck, Phys. Rev. **52** (1937) 54.

[13] J. Küblbeck, M. Böhm and A. Denner, Comput. Phys. Commun. **60** (1990) 165;
H. Eck and J. Küblbeck, *Guide to FeynArts 1.0*, University of Würzburg, 1992.

[14] T. Hahn and M. Perez-Victoria, Comput. Phys. Commun. **118** (1999) 153 [hep-ph/9807565];
T. Hahn, Nucl. Phys. Proc. Suppl. **89** (2000) 231 [hep-ph/0005029].

[15] S. Dittmaier and M. Krämer, Phys. Rev. D **65** (2002) 073007 [hep-ph/0109062].

[16] R. Mertig, M. Böhm and A. Denner, Comput. Phys. Commun. **64** (1991) 345;
R. Mertig, *Guide to FeynCalc 1.0*, University of Würzburg, 1992.

[17] S. Dittmaier, Phys. Rev. D **59** (1999) 016007 [hep-ph/9805445].

[18] S. Dittmaier, Nucl. Phys. B **565** (2000) 69 [hep-ph/9904440].

[19] F. Jegerlehner, Z. Phys. C **32** (1986) 195.

[20] U. Baur, S. Keller and D. Wackeroth, Phys. Rev. D **59** (1999) 013002 [hep-ph/9807417].

[21] J. Kripfganz and H. Perlt, Z. Phys. C **41** (1988) 319;
H. Spiesberger, Phys. Rev. D **52** (1995) 4936 [hep-ph/9412286].

[22] W. J. Stirling, talk given at the workshop *Electroweak Radiative Corrections to Hadronic Observables at TeV Energies*, Durham, UK, September 2003.

[23] T. Kinoshita, J. Math. Phys. **3** (1962) 650;
T. D. Lee and M. Nauenberg, Phys. Rev. **133** (1964) B1549.

[24] K. Hagiwara *et al.* [Particle Data Group Collaboration], Phys. Rev. D **66** (2002) 010001.

[25] F. Jegerlehner, DESY 01-029, LC-TH-2001-035 [hep-ph/0105283].

[26] H. L. Lai *et al.*, Phys. Rev. D **55** (1997) 1280 [hep-ph/9606399].

[27] A. Sirlin, Phys. Rev. D **22** (1980) 971.

[28] M. Roos *et al.*, Phys. Lett. B **111** (1982) 1.

[29] S. Sarantakos, A. Sirlin and W. J. Marciano, Nucl. Phys. B **217** (1983) 84.